A new conceptual approach for systematic error correction in CNC machine tools minimizing worst case prediction error.

A NEW CONCEPTUAL APPROACH FOR SYSTEMATIC ERROR CORRECTION IN CNC MACHINE TOOLS MINIMIZING WORST CASE PREDICTION ERROR

N. V. Chung[1], Erik L. J. Bohez[1] , G. Belforte[2], H.T.Phong[3]

[1] Asian Institute of Technology, Thailand

[2] Politecnico Di Torino, Italy

[3] Ho Chi Minh City International University, Vietnam

Abstract

A new artifact based method to identify the systematic errors in multi-axis CNC machine tools minimizing the worst case prediction error is presented. The physical artifact is manufactured on the machine tool and later measured on a Coordinate Measuring Machine. The artifact consists of a set of holes at locations that minimize the worst case prediction error. The physical artifact in the experiment contained multiple virtual artifacts. This allowed to separate the random errors from the systematic errors and assess their relative magnitude. Also there was no additional random set up error for each atifact due to the combination in a single physical part. The result of the measurements is then used to compute the systematic error approximated as 5^{th} degree polynomials. A case study on a vertical milling machine is used to verify the new approach. It is observed that the degree can be lowered to three without reducing the systematic error estimates. The obtained results are very promising. The method is inherently simple and required only a short time to produce the artifact. The method is very simple because of three reasons. First only the six components of the closed loop systematic error are measured directly. Secondly because the artifact consist only of producing holes. Thirdly because everything indicated that third degree polynomial are sufficient, the numbers of holes required per machine axis can be further reduced from 6 to 4.

Multi-axis CNC, systematic error, optimal sampling, Minimal worst case prediction error.

1 INTRODUCTION

The main idea underlying this research line is quite simple and follows from the consideration that, when a CNC machine is affected by systematic errors such errors can be in principle identified and corrected via software, moving the CNC machine axis in such a way that compensates for the systematic errors. Provided that the error identification procedure is not too complex and cumbersome, this approach is appealing for two main reasons: (i) this procedure can be much cheaper than a hardware correction and tuning of the different slides along which or around which the motion of the CNC machine axes occur; (ii) this procedure can be repeated in time whenever it is perceived that a check of the machine accuracy is needed.

In order to identify the systematic errors, the approach we are proposing foresees to mill one or more suitable artifacts with the machine to be corrected. As a matter of fact the systematic errors will be reflected in a systematic difference between the milled artifact and the nominal designed work piece. If the artifact is then measured with an accurate measuring machine it should be possible to detect such differences. These last enable to identify the systematic errors, provided that a suitable model for them is available so that, finally, errors can be corrected using the identified model.

Actually in a previous study [4] some experimental results related to the identification of angular errors and their possible correction have been presented. The solution proposed was based on an optimal selection of measurements which minimizes the uncertainties of the derived estimates. Such solution, however, does not minimize the prediction error, which is the difference between the true unknown error function to be corrected and its estimate which is derived from the measurements. Indeed the prediction error is the one in which we are most interested in, since it is the one that we commit when we use estimated corrections. With the procedure described in [4] such error turns out to be quite consistent. For this reason a new experimental setting targeting the prediction error containment was designed and preliminary tested to evaluate its feasibility.

Aim of this paper is to present the results of this test describing the general framework of the suggested procedure and presenting the outcomes of the experiments we have conducted.

2 BACKGROUND

For the self-consistency of this paper the geometric error correction problem is outlined first, evidencing different approaches that can be followed and motivating the direction in which the following investigation is conducted. Relevant theoretical results needed for the definition of the error correction procedure are then presented in a concise but comprehensive way.

2.1 The problem of geometric error correction

The accuracy of milling machines is indeed related to several different factors that include geometric errors, dynamic effects related to the forces applied in the milling process, thermal deformations etc. [5] Geometric errors in particular

present systematic components deriving from the real structure of the machine in which the movements of the different slides do not follow the ideal path they should, but slightly deviate from it. The usual approach to correct such errors consists in measuring, for each axis of the CNC machine, the six elementary error components that can be associated to the movements of any rigid body (three linear errors along three reference axes and three rotations around the same three reference axes) and then correcting the hardware of the machine accordingly. The different approach outlined in [1] consists in focusing on the total closed loop volumetric error in the working space of the machine. Such error, which describes the position and orientation error of the tool with respect of the work piece, has in general six components: three linear components of the position of the cutting tool (dx, dy, dz) and three angular components of its orientation (di, dj, dk). Indeed these total error components are functions of the n axes coordinates since they are the result of the combined effect of the elementary error components associated to the movement of each CNC machine axis. Note that, from a practical point of view the end user is only interested in the six total closed loop volumetric error components (and indeed in their correction) and not in the elementary error components relative to each axis. The goal is then to identify such total error components in order to correct them not in the hardware, but in the software of the machine. In fact, if the total error function is known throughout the working space, a suitable correction to compensate for such systematic error can be added at any location in the working space. The practical implementation of the correction can be embedded in the control unit of the CNC machine or it can be carried out during the post-processing while generating the g-code to be feed to the machine.

In order to derive the total closed loop volumetric error components two approaches are possible in principle. The first one foresees the independent identification (with suitable measurements) of each elementary error component affecting the movement of each slide of the CNC machine. Such elementary components are then combined together to get the six components of the total error. The second approach consists in directly identifying, from suitable measurements, each one of the six components of the total closed loop volumetric error. Here we focus on this second approach.

In order to measure any of the six components of the total error at any location in the working space of the CNC machine, two approaches are again possible. The first one foresees the use of suitable measuring equipment which allows to determine, with high accuracy, the position of the tool in the spindle. There is a patent [6] which is based on this kind of approach, while some considerations in this direction are presented in [1]. The second possibility is to measure the total closed loop volumetric error components from the differences that a suitable artifact milled with the CNC machine to be corrected has with respect to its nominal shape [2,3]. Remark that in this case the derivation of the error measurement is performed in two distinct steps. In the first one the artifact is milled with the CNC machine while in the second the artifact is measured with a measuring machine. These two steps do not need to be done at the same time and in the same location. This fact provides consistent flexibility since there is no need to have an (expensive) measuring machine in the same location as the CNC machine to be corrected. On top of this no particular skills are needed for the milling of the artifact. These practical considerations suggest that the use of artifacts for deriving total errors in CNC machines could lead to simple and relatively cheap procedures that would be of great industrial interest, provided that the obtained corrections are satisfactory. The goal of the research presented here is to contribute to the analysis of the quality of corrections that can be obtained with this kind of approach. However some important points which concur to precisely define the correction procedure have to be addressed first and are reported in the following.

2.2 Modeling of the total closed loop volumetric error components

In order to allow for total error correction a suitable model for it needs to be chosen. In this regard it should be noted that each one of the six elementary error components associated with the movement of a single slide in a CNC machine depends only on the moving slide coordinate. Furthermore such error components which depend on the imprecise realization of the real slide, are small and slowly varying in a rather unpredictable way. For this reason such elementary error components are perceived to be reasonably modeled by monodimensional polynomial functions of the varying coordinate. Also in three coordinate measuring machines the eighteen elementary error components affecting the motion of their three axes (three linear and three rotary error components for each axis) are commonly modeled as polynomials and fifth order polynomials are usually chosen as they are considered appropriate to take into account systematic errors. For what concerns the modeling of the six total closed loop volumetric error components, which are the combined results of the elementary error components affecting the motion of each CNC slide, it follows that they can be satisfactorily approximated by suitable polynomial functions of the n moving joint coordinates. This indeed is a typical assumption widely discussed in [1] that is also used in other studies like in [6] [7]. The structure of such multidimensional polynomials depends on the layout of the machine that includes the number and relative position of linear and rotary axes which affect the way in which elementary error functions combine together into the total error components. Their determination is a rather straightforward exercise if second order terms are neglected. This simplification is commonly used since the errors are assumed to be small. In [1] the complete derivation is shown for 5-axis milling machines of one of the most common structures. In general the n-dimensional polynomials in the n joint coordinates describing the total errors of a n-axis CNC machine are not complete, but they include monomials which are function of at most two different joint coordinates one of which is at most of degree one. Note that for the spindle orientation errors (total angular errors) the polynomial functions representing them are the sum of n monodimensional polynomials in the n coordinates of the n axes of the CNC machine [1].

2.3 “Best” identification setting for the error determination

Once the polynomial model structure of total closed loop volumetric errors is assumed according to the considerations reported in previous section, it is possible to look for the best identification setting for the estimation of the parameters of the polynomials from a suitable set of measurements of the error functions.

Two problems have to be solved to implement the identification. The first one, which is more practical, consists in finding out a procedure that enables to measure the total closed loop volumetric errors throughout the working space of the CNC machine at given points identified by the values of the n joint coordinates. The second one, which is more theoretical, consists in finding out which are the most convenient values of the n joint coordinates where the error functions should be measured. These two problems are analyzed in the following.

The procedure that enables to measure one of the total error components for a given value of the n joint coordinates is more related to practical aspects connected with the way in which such measurements have to be carried on. Recall that we are supposed to mill an artifact according to nominal values of a model, Such artifact is then measured with a high precision measuring machine. The results are then compared with the nominal shape of the artifact to derive the errors. What is needed is then a geometric figure that can be easily milled in the artifact so as to provide information about the position in which it was milled together with indications on the orientation of the spindle. Such geometric figure needs also to be easily measured. One simple but effective shape consists in cylindrical holes which can be easily milled. As a matter of fact the central axis of the hole provides the information about the orientation of the spindle, while the intersection of its central axis with the bottom plane of the hole, or with the plane on which the hole has been drilled, or with any other suitably defined plane, provides the information about the coordinates where the hole has been milled. All these quantities can be easily measured with a measuring machine and compared with the nominal ones of the mathematical model of the artifact, thus providing the required information about the value of the six total closed loop volumetric error components at that location.

For what concerns the selection of the sampling points were the total error functions have to be evaluated in the n-dimensional space of the joint coordinates, it should be noted that in an error free ideal condition any set of at least p independent measurements (where p is the number of parameters to be identified) would enable the derivation of the exact values of the parameters and consequently of the error functions throughout the working space of the CNC machine. This would enable to fully correct the systematic errors. However, in the real world, measurements are not error free, moreover CNC machines have some small randomness in their movements which adds extra errors. All these errors, that jointly act as measurement errors, induce uncertainties on the estimates of the parameters of the polynomials describing the total errors. It follows that, when the total errors are evaluated in any point of the workspace of the CNC machine using the estimated polynomials, a prediction error is committed that is the difference between the (unknown) true value of the error and the one computed using the estimated polynomials. In order to reduce parameter uncertainties and consequently the prediction error the usual approach consists in collecting a large amount of measurements. In our case, however, measurements are quite expensive in terms of time required for their execution as well as in terms of equipment. This fact imposes serious constraints since for increasing number of measurements the calibration procedure becomes less appealing from a practical point of view. Therefore the number of measurement points should be kept as low as possible and the collection of a large amount of measurements is not a feasible solution. A careful analysis of the selection of the sampling points turns out to be an unavoidable step because, for a fixed number of measurements, the parameter uncertainties as well as the prediction error are functions of the location where the measurement are collected.

The selection of the most convenient sampling points can be accomplished making use of results obtained in the field of optimal experiment design [8], [9], [10]. These results were developed in the set membership error context, when measurement errors are not statistically characterized but they are assumed to be described by tolerances. Actually the concept of tolerances fits pretty well in the mechanical setting in which CNC machines are usually operated. Note, however, that available results are mainly related to the reduction of the uncertainty in the parameter estimates. Little results are available for the reduction of the prediction error that is the most important in connection with the correction of systematic errors in CNC machines.

2.4 Set membership identification and optimal experimental design

The main results for optimal experiment design have been derived for monodimensional functions $F(\theta,t)$ of the scalar variable t which are linear in the parameter vector $\theta=[\theta_0\ \theta_1\ \theta_2\ \dots\ \theta_p]$ to be estimated. In general $F(\theta,t)=\theta_0 f_0(t)+\theta_1 f_1(t)+\theta_2 f_2(t)+\dots+\theta_p f_{p-1}(t)$, where $f_i(t)$ i=0…p-1, are p given linearly independent functions. Indeed polynomials represented according to the Vandermonde base have this kind of structure in which $f_i(t)=t^i$, i=0…p-1. It is assumed that measurements of such functions are affected by an error e(t) which is known to be bounded so that $|e(t)|\le E$. Remark that this assumption does not require any statistical assumption on the error although it does not exclude that the error is a stochastic variable.

Whenever m measurements are collected at m different sampling times $t_1,t_2,\dots,t_m$ with $m\ge p$, so that there are at least as many measurement as parameters, and the matrix

$$A(t_1,t_2,\dots,t_m,)=\begin{bmatrix} F_0(t_1) & F_1(t_1) & \cdots & F_{p-1}(t_1) \\ F_0(t_2) & F_1(t_2) & \cdots & F_{p-1}(t_2) \\ \vdots & \vdots & \vdots & \vdots \\ F_0(t_m) & F_1(t_m) & \cdots & F_{p-1}(t_m) \end{bmatrix} \qquad (1)$$

is full rank, then It is possible to derive an estimate for the parameter vector θ together with its uncertainty which depends on the bounds E on the measurement error, on the choice of the sampling times $t_1,t_2,\dots,t_m$, and on the error realization. Note that in the case of monodimensional polynomials matrix A is full rank whenever the measurement points are distinct.

Whenever it is provided a set $T=\{t_1, t_2, \ldots, t_m\}$ of possible sampling times at which function $F(\theta,t)$ could be measured, it is possible to compute the corresponding Worst Case Uncertainty which is the largest uncertainty, with respect to any possible error realization, which can affect the parameter estimates derived from the measurements collected at the T sampling times. Meanwhile the corresponding optimal sampling set (or optimal sampling schedule) T_O, which is a subset of T, can also be derived. The optimality of such set consists in the fact that its Worst Case Uncertainty is the same of set T. Therefore using only the measurements in T_O it is ensured that the actual parameter uncertainties, in the worst case, will be the same as that achieved using all the measurements T.

Remark that no actual measurements are needed to compute the Worst Case Uncertainty and the set T_O. It is also important to note that set T_O has a number of elements that is bounded between p and p^2. Whenever the number of elements in T_O is equal to p, then the set is referred to as minimum worst case.

For complete polynomials in the Vandermonde base in which $F(\theta,t)= \theta_0+\theta_1 t+\theta_2 t^2+\ldots+ \theta_{p-1}t^{p-1}$ the optimal sampling set T_O is minimum worst case. In the case in which the set T is constituted by the infinite sampling times of an interval $[t_a,t_b]$ the optimal sampling set can be analytically derived [9] [10] and it is given by the values at which the 1st kind Chebyshev polynomial of degree p-1 associated with the interval $[t_a,t_b]$ achieves its minimal and maximal values.

Little results are available for the case of multidimensional functions $F(\theta,t)$, when variable t is a vector with n components. This is actually the case of interest for CNC machine error correction since the total closed loop volumetric errors are modeled with multidimensional polynomials in the n joint coordinates, x,y,z,A,B. Unfortunately no close form results are available for generic multidimensional polynomials for which, only the numerical computation can be used. This can lead to several practical problems related to the fact that the number of possible candidate measurements, which are the nodes of a n-dimensional grid, can be very large and numerical algorithms can sometimes derive a suboptimal sampling schedule T_{SO} whose elements are still bounded between p and p^2, but are more than those of T_O, so that $T_{SO} \supseteq T_O$.

All results presented so far focus on the reduction of the uncertainty in the parameter estimates. For what concerns the reduction of the worst case prediction error the main result available so far is, to the best of our knowledge, relative to monodimensional polynomials of degree p-1, when a set T of only p sampling points over a finite interval $[t_a,t_b]$ has to be chosen. In this case according to a conjecture by Bernstein [11] which has been proved by Kilgore [12] and De Boor – Pinkus [13] the minimum worst case prediction error function is a piecewise polynomial that has one local maximum on each interval $[t_i,t_{i+1}]$ (with $t_{i+1} > t_i$, $i=1,\ldots,p-1$). The sampling schedule for which the maximum of the prediction error over the interval $[t_a,t_b]$, which is the worst case prediction error, is minimized is the one for which the local maxima on each interval $[t_i,t_{i+1}]$ are equal. Unfortunately no closed form is available for such schedule which can be only numerically derived. However the schedule is well approximated by the roots of the Chebyshev polynomial of first kind translated on the interval $[t_a,t_b]$ of interest.

For what concerns prediction errors for multidimensional polynomials it appears that a gridding over the whole working space is unavoidable if worst case prediction error has to be contained. Indeed this requirement induces practical problems since the number of required points increases exponentially with the number of dimensions. It should also be noted that while the sampling schedule is selected so as to ensure a sufficiently small worst case prediction error, once that actual measurements are collected according to that same schedule and their number is larger than the number of parameters to be estimated, then the actual prediction error (as well as the actual uncertainties of the parameter estimates) will be, in general, smaller than the worst case one. Our conjecture is that the gridding which is obtained choosing for each dimension the optimal sampling schedule minimizing the monodimensional worst case prediction is optimal for multidimensional polynomials which are the sum of monodimensional polynomials and almost optimal for other multidimensional polynomial structures. Preliminary numerical results do sustain this conjecture which is the pillar of patent [3].

3 ESPERIMENTAL FEASIBILITY STUDY OF SYSTEMATIC ERROR CORRECTION

3.1 Goals and framework of the experimental feasibility study

In the light of the results reported above, it appears advisable to carry on a preliminary feasibility study to examine the possibility to recognize, with the proposed approach, systematic errors in CNC machines, to get more insight on the uncertainties that the measurement procedure can induce, and to have some information on the repeatability of the procedure. To facilitate the execution of the test, still getting valuable information, it is convenient to carry on the study on a CNC machine deserving moderate accuracy to avoid the risk that a very accurate CNC machine prevents the possibility to detect systematic errors. At the same time, since the number of required measurements increases with the number of axes in the CNC machine and so does the experimental setting complexity, it appears advisable to carry on the study testing the workspace relative to a low number of axes. The choice of a two axis environment appears to be a convenient compromise between simplicity and meaningfulness of the study.

Indeed for the two dimensional space a numerical analysis of the worst case errors can be carried our evidencing some interesting features also in comparison with previous results presented in [4].

3.2 Analysis of the worst case identification and prediction errors for in the two dimensional space

In order to provide a comprehensive framework for our experiments, the functions used for modeling the total closed loop volumetric errors in the two dimensional case are derived in the following and some a priori analysis on the optimal sampling selection for such functions and on the prediction error that can be achieved are presented as well.

The CNC milling machine we are dealing with is actually a three axis machine (X-Y-Z) of which only the two dimensional working space X-Y is considered.

The total closed loop volumetric errors can be easily derived as functions of the elementary error functions associated with the movements of the three slides (X-Y-Z) of the CNC machine. They can be easily obtained particularizing the relation presented in [1], which are derived for a 5 axis milling machine, deleting the terms relative to the two rotary axes. It results that

$$
\begin{aligned}
dx &= T_{XX} + T_{YX} + (R_{XZ} - S_{YZ})Y + (R_{YY})Z \\
dy &= T_{XY} + T_{YY} - R_{XZ}\,X - (R_{XX} + R_{YX} - R_{ZX})Z \\
di &= R_{XY} + R_{YY} \\
dy &= -R_{XX} - R_{YX}
\end{aligned}
\qquad (2)
$$

Where T represents an elementary translational error and R represents an elementary angular error. The first subscript accounts for the moving axis which is the variable on which the elementary error function depends, while the second subscript indicates either the direction along which the translational error occurs or the axis around which rotarational errors occurs. Positive rotation is defined by the right-hand rule. Squareness errors are indicated with S and are constants.

For example

T_{XY} Translational error of X-body in Y direction in function of X position

R_{xz} Rotational error of X-body around Z-axis in function of X position

SYZ Squareness errors of the y-axis around z-axis

If the elementary translational and rotational error functions are represented as fifth degree polynomials, beside function R_{XZ} which is assumed to be represented by forth degree polynomial, and keeping in mind that Z is assumed to be constant, it follows that:

$$
\begin{aligned}
dx &= \theta_{x0}+\theta_{x1}X+\theta_{x2}X^2+\theta_{x3}X^3+\theta_{x4}X^4+\theta_{x5}X^5+\theta_{x6}Y+\theta_{x7}Y^2+\theta_{x8}Y^3+\theta_{x9}Y^4+\theta_{x10}Y^5+\theta_{x11}XY+\theta_{x12}X^2Y+ \\
&\quad \theta_{x13}X^3Y+\theta_{x14}X^4Y+\theta_{x15}X^5Y \\
dy &= \theta_{y0}+\theta_{y1}X+\theta_{y2}X^2+\theta_{y3}X^3+\theta_{y4}X^4+\theta_{y5}X^5+\theta_{y6}Y+\theta_{y7}Y^2+\theta_{y8}Y^3+\theta_{y9}Y^4+\theta_{y10}Y^5 \\
di &= \theta_{i0}+\theta_{i1}X+\theta_{i2}X^2+\theta_{i3}X^3+\theta_{i4}X^4+\theta_{i5}X^5+\theta_{i6}Y+\theta_{i7}Y^2+\theta_{i8}Y^3+\theta_{i9}Y^4+\theta_{i10}Y^5 \\
dj &= \theta_{j0}+\theta_{j1}X+\theta_{j2}X^2+\theta_{j3}X^3+\theta_{j4}X^4+\theta_{j5}X^5+\theta_{j6}Y+\theta_{j7}Y^2+\theta_{j8}Y^3+\theta_{j9}Y^4+\theta_{j10}Y^5
\end{aligned}
\qquad (3)
$$

Remark that if the elementary error function R_{XZ} is also assumed to be a fifth order polynomial an extra term $\theta_{y11}X^6$ would be present in dy. In such condition the parameters of the dy functions would be no longer identifiable from measurement obtained on a 6x6 grid. A 6x7 grid would be necessary. It has therefore been chosen to assume that function R_{XZ} is adequately described by a forth degree polynomial.

As it can be seen, dx, di and dj are the sum of two fifth degree polynomials one in X and the other in Y, while dx has also the terms resulting from a fifth degree polynomial in x multiplied by Y.

A result that will be published in the future allows to state that for the case in which the total error function is the sum of two monodimensional polynomials one in X and the other in Y, when the values of X and Y at which the function can be measured are bounded to belong to given intervals, then the optimal sampling schedule, which is not available in closed form, can be numerically derived considering only, as candidate measurements, the nodes of the gridding that, in each dimension, has the monodimensional optimal sampling of the monodimensional polynomial in that same dimension.

When the values of X and Y at which the function can be measured are both bounded in the normalized interval [0,1] the nodes of the grid on which the optimal sampling can be numerically sought is immediately derived since the optimal sampling for a monodimensional polynomial of fifth degree on the interval [0,1] is given by the values {0.0000 , 0.0955 , 0.3455 , 0.6545 , 0.9045 , 1.0000}. In the following we will refer to this grid as the optimal parameter estimation grid.

Note that instead the values which define, on the same interval [0,1], the p coordinates which allow to minimize the worst case prediction error are given by the values {0.0000 , 0.1340 , 0.3660 , 0.6340 , 0.8660 , 1.0000}. Also these values can be used to derive a two dimensional grid which should be (almost) optimal for what concerns the prediction error. the following we will refer to this grid as the optimal prediction error grid.

In this simple case in which the optimal parameter estimation grid consists of only 36 points, it can be tested, by exhaustive search of all the combinations of 11 sampling points (as many as the parameters), if the functions dy, di, and dj are minimum worst case so that their optimal sampling schedule consists of only 11 sampling points. It turns out that the functions have two distinct\ optimal sampling schedules. This is a rather new finding since monodimensional polynomials in general have only one optimal sampling schedule. Note also that if the dimension of the space is higher than 2, the number of points on the gridding increases to such an extent that it prevents the exhaustive search and then the optimal sampling schedule can be derived only with procedures based on linear programming as illustrated in [4]. In such condition, however, only suboptimal sampling schedules have been found already for the three dimensional case [4].

A further remark on the optimal sampling schedule is that it is sensitive to changes in the interval on which measurements can be collected. If the intervals on which X and Y are bounded to vary are both in the interval [1,2], it results that no minimum worst case sampling schedule is available for functions dy, di, and dj. This can be explained by the fact that a shift in the intervals is equivalent to a change in the base that is used for representing the polynomials and the optimal

sampling is sensitive to base changes, as discussed in [14]. On the contrary a change in scale does not affect the optimal sampling schedule.

Note that normalizing the measurement error bounds to one so that $|e(t)| \leq E=1$, the worst case prediction error that can be achieved within the normalized working space [0,1]x[0,1] with the two optimal schedules which have been derived results to be 9.00 and 8.44 respectively (which is almost one order of magnitude greater than the measurement error bound). Such worst case prediction error drops instead to 1.99 if all the 36 points of the optimal parameter estimation grid are used, and it drops further to 1.68 if the optimal prediction error grid is used. On the contrary the worst case prediction error rises to 3.11 if a uniform gridding is used. Note that in any case, the actual prediction error should be smaller than the worst case one since the used measurements are more than the parameters to be estimated.

For function dx the worst case prediction error that is achieved using all the 36 measurements of the optimal parameter estimation grid is equal to 2.13 that drops to 2.06 if the optimal prediction error grid is used, while it rises to 4.34 if an uniform gridding is adopted.

3.3 The artifacts

The practical experiment was conducted on an EMCO VMC200 CNC machine whose workspace is as follows: X-axis traverse 420mm; Y-axis traverse 330mm; Z-axis traverse 400mm. The maximal dimensions that a artifact can have are: (LWH) 400 x 300 x 190mm. It is chosen to work only on a workspace (X,Y) of 350 x 250mm which is centered in the total workspace of the machine. In such condition the nominal positions of the 36 holes to be milled are reported in the following Table 1 while in Figure 1 the layout of the holes in the artifact is depicted.

The workpiece is constituted by a solid piece of RAKU-TOOL MB- 0670 resin with the following dimensions (LWH) 400 x 300 x 70mm and a weight of about 7,5Kg. The height of the work piece is relatively large to prevent deformation of the work piece during clamping on the CNC machine and during transportation. The thermal expansion coefficient of this material is 50 10^{-6} / ºC.

So a length of 1000 mm will expand 50µm per ºC. As the largest distance between the holes is about 350 mm there will be considerable thermal expansion (17.5 µm) if the temperature is not kept constant. So when producing and measuring the artifact it is necessary to make sure that it has reached the equilibrium temperature of the machine tool environment and the CMM environment. If the temperature between producing and measuring the artifact is stable but different corrections can easily be computed. A metal artifact would have about 10 times lower expansion but is would be heavier and cutting forces would be considerable higher.

The 36 holes are milled in series, in the same sequence in which they are reported in Table 1, by a flat end mill with a diameter of 10mm, for a depth 15mm. A simple CNC program controls the whole milling process.

Minimal three identical artifacts were considered necessary to asses the relative magnitude of the systematic error relative to the random error. It was realized that this could be done in a single real workpiece by just shifting the workpiece on the machine table and running the same CNC program. This assured that the holes were at the same absolute location in the machine tool workspace. Workpiece and tool offsets need to be the same for each of the three artifacts so that the error can be referred to the machine coordinate system. The procedure to produce the three artifacts in one part is given below.

1. Put the workpiece on the CNC machine with its sides aligned with the axes of the machine. Clamp the workpiece on the CNC machine and mill with the CNC program a first series of 36 holes. Such series of holes constitutes the first artifact.
2. Unclamp the workpiece and shift it on the machine table along the y axis applying a shift of -11.5mm. Clamp the workpiece again on the CNC machine and mill with the CNC program a second series of 36 holes. Such series of holes constitutes the second artifact.
3. Unclamp the workpiece and shift it on the machine table along the x axis applying a shift of 15mm. Clamp the workpiece again on the CNC machine and mill with the CNC program a third series of 36 holes. Such series of holes constitutes the third artifact.

The shifting accuracy is not important as the hole 1 and the hole 31 will be used to align the origin and the x axis of the three artifacts.

Figure 2 shows the workpiece in the milling phase with the different series of holes constituting the different artifacts.

Table 1. Coordinate of points on 2D artifact (Nominal)

Points	X	Y	Points	X	Y
1	25	25	19	254.075	25
2	25	48.875	20	254.075	48.875
3	25	111.375	21	254.075	111.375
4	25	188.625	22	254.075	188.625
5	25	251.125	23	254.075	251.125
6	25	275	24	254.075	275
7	58.425	25	25	341.575	25
8	58.425	48.875	26	341.575	48.875
9	58.425	111.375	27	341.575	111.375
10	58.425	188.625	28	341.575	188.625
11	58.425	251.125	29	341.575	251.125
12	58.425	275	30	341.575	275
13	145.925	25	31	375	25
14	145.925	48.875	32	375	48.875
15	145.925	111.375	33	375	111.375
16	145.925	188.625	34	375	188.625
17	145.925	251.125	35	375	251.125
18	145.925	275	36	375	275

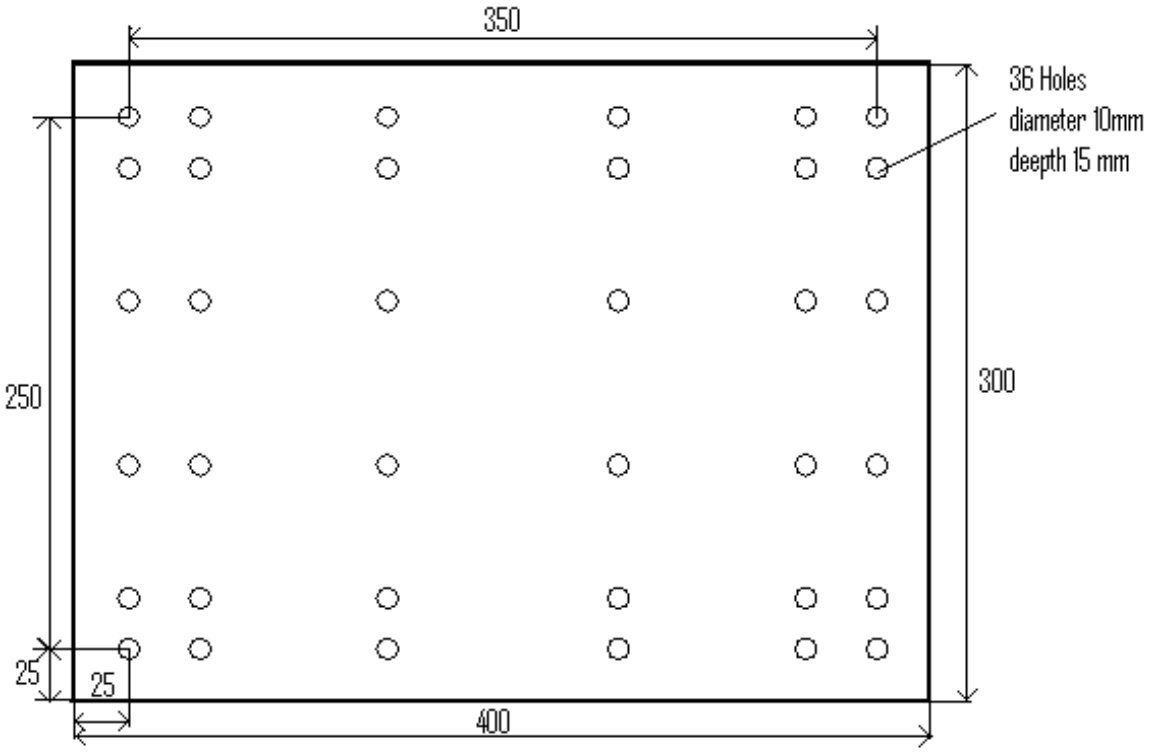

Figure 1 : The workpiece with the holes of the first series constituting the first artifact

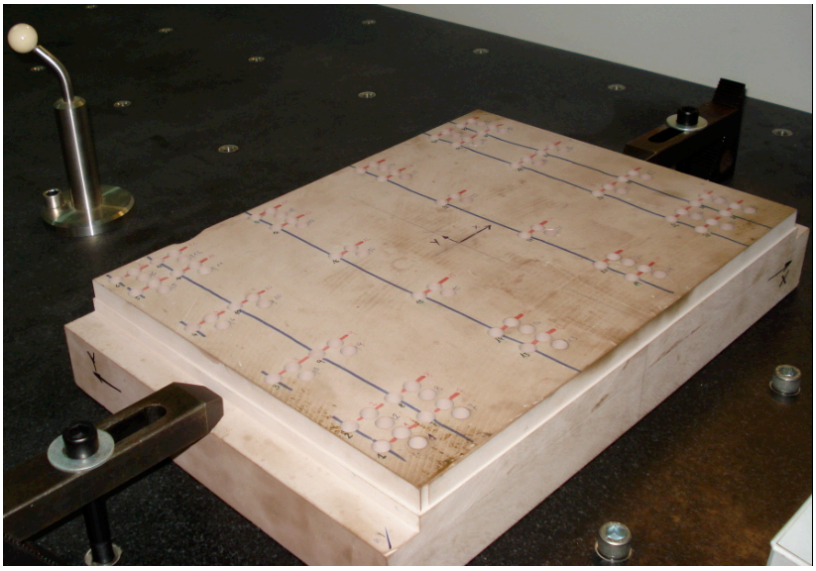

Figure 2: Artifact manufacturing on Milling

3.4 The measurement of the workpiece

The three series of holes constituting the three different artifacts in the same work piece are measured on a Zeiss CMM according to the following procedure. The workpiece is first clamped on the CMM table with its sides manually aligned with the axes of the CMM as depicted in Figure 3. in particular the edge near hole 1 and 31 is aligned as precise as possible with the X-axis of the machine. The CMM machine is calibrated and thereafter all the three series of 36 holes, which constitute the three artifacts are sequentially measured without any change in the coordinate system.

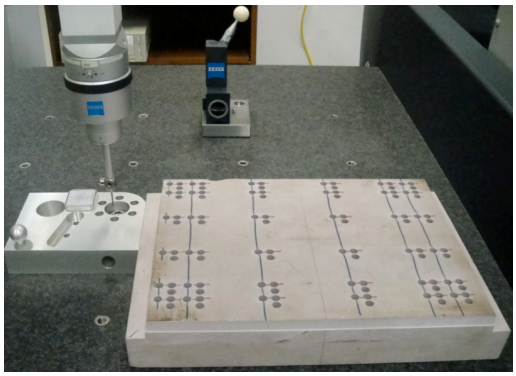

Figure 3: Measuring workpiece on Zeiss CMM

For each hole in the workpiece 96 measurements are carried on. In particular, moving only one axis of the CMM at a time, the extreme points of two perpendicular cords (which are chosen so as to be as close as possible to diameters) on a plane 2mm inside the hole are measured 10 times each, for a total of 40 measurements. The same is done on a second plane 12mm inside the hole for other 40 points. Then 8 points on the bottom plane of the hole are measured twice. The scheme of the total 96 measurement points is reported in Figure 4. The raw data of the 96 measurement points in one single hole are reported for reference in the following Table 2.

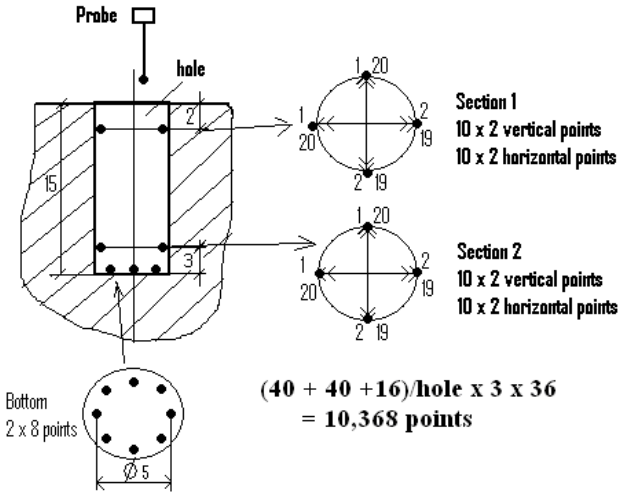

Figure 4: Layout of the 96 measurement points in one single hole of the artifact

Table 2: Series of measurement data of one hole

x	y	Z	X	y	z	x	y	z
20.0813	25.0055	-2.0001	25.0073	30.1083	-2.0018	25.0066	30.1095	-12.0014
30.0959	24.9913	-1.9966	24.9895	20.092	-1.9961	24.9903	20.1021	-11.9954
20.0812	25.0056	-2.0001	25.0059	30.1083	-2.0019	25.0068	30.1095	-12.0017
30.0958	24.9903	-1.9964	24.9897	20.092	-1.9959	24.9902	20.1021	-11.9951
20.0811	25.0058	-1.9993	25.0063	30.1083	-2.0019	25.0064	30.1094	-12.0017
30.0958	24.9914	-1.9965	24.9896	20.0921	-1.996	24.9895	20.1021	-11.9954
20.0811	25.0053	-1.9999	25.0063	30.1084	-2.0021	25.0062	30.1094	-12.0014
30.0958	24.9913	-1.9973	24.9897	20.092	-1.9962	24.99	20.102	-11.9952
20.081	25.006	-2.0001	20.0918	25.0068	-11.9998	25.0065	30.1094	-12.0015
30.0958	24.9915	-1.9966	30.0974	24.9936	-11.997	24.9903	20.102	-11.9956
20.081	25.0055	-1.9995	20.0917	25.007	-11.9989	25.0066	30.1094	-12.0018
30.0958	24.9916	-1.9967	30.0974	24.9927	-11.9967	24.9898	20.102	-11.9954
20.0809	25.0059	-1.9999	20.0917	25.0071	-11.9994	25.0071	30.1094	-12.0018
30.0957	24.9917	-1.9965	30.0975	24.9928	-11.9967	24.99	20.102	-11.9955
20.0809	25.0058	-2.0001	20.0917	25.0067	-11.9993	25.0067	30.1094	-12.0016
30.0957	24.9909	-1.9969	30.0974	24.9918	-11.997	24.9895	20.102	-11.9955
20.0808	25.006	-2.0003	20.0916	25.0067	-11.9996	22.4994	24.9983	-14.992
30.0957	24.9915	-1.9968	30.0975	24.9922	-11.9972	23.2288	26.7717	-14.9874
20.0808	25.0051	-2.0003	20.0917	25.007	-11.9991	24.9972	27.4996	-14.9815
30.0956	24.9917	-1.9965	30.0975	24.9917	-11.9971	26.7679	26.7707	-14.9783
25.0073	30.1083	-2.0019	20.0917	25.007	-11.9994	27.4978	24.9995	-14.9816
24.9902	20.0924	-1.996	30.0976	24.9924	-11.9968	26.7709	23.2311	-14.9863
25.0065	30.1084	-2.0021	20.0917	25.0071	-11.9997	25.0004	22.5003	-14.9934
24.9895	20.0923	-1.9961	30.0977	24.9922	-11.997	23.2309	23.2298	-14.9943
25.007	30.1085	-2.0019	20.0918	25.007	-11.9995	22.5006	24.9985	-14.9927
24.9882	20.0923	-1.9961	30.0977	24.9921	-11.9969	23.2282	26.7711	-14.9879
25.0072	30.1085	-2.0021	20.0919	25.0072	-11.9995	24.9963	27.4997	-14.9821
24.9902	20.0922	-1.996	30.0978	24.9926	-11.9969	26.7676	26.7723	-14.9789
25.0064	30.1083	-2.0017	25.0084	30.1094	-12.0013	27.4972	25.0002	-14.9824
24.9887	20.0922	-1.9961	24.9889	20.1022	-11.9955	26.7707	23.2311	-14.9866
25.0058	30.1083	-2.0019	25.0071	30.1095	-12.0014	25.0003	22.4997	-14.9938
24.9897	20.0921	-1.996	24.9894	20.1022	-11.9953	23.2305	23.2313	-14.9947

3.5 Measurement elaboration

The location, in the X-Y plane as well as the orientation of each one of the 36 holes in each artifact should be derived from the measurements. This can be obtained deriving the center line of the holes which provides the information on their orientation (and therefore on the orientation of the tool that milled them). The intersection of the center line with any suitable plane provides then the information on the hole positions.

For each hole the first 40 measurements allow to derive the center of the hole on one plane which is 2 mm inside the hole. while the second 40 measurements allow to derive the centre of a second plane 10 mm deeper. Redundant measurements have been collected so that the random measurement error can be reduced. Since the measurements are collected, with the precision allowed by the measuring machine, as the extreme points of two perpendicular cords in the directions of the X-Y axes of the measuring machine and are very closed to two diameters of the circumference to be measured, the (x,y) coordinates of the centre have been just computed taking the average of the 20 measurements of the extremes of each cord.

In order to identify the X-Y location of the holes it has been decided to use the centers on the plane 2 mm inside the hole. The measurements of the bottom plane of the hole have not been used as the varied quite a lot in the z coordinate.

Once the two centers on the two planes have been computed for each hole of an artifact, in order to represent them in the nominal reference coordinate system, a translation has been applied to all of them in order to shift the axis origin in the center of hole 1 at 2 mm level. A rotation around the z axis has then be applied in order to let the x axis pass through the center, at 2 mm level, of hole 31. Once these transformation have been applied the comparison with the nominal values of the holes has been carried on deriving the errors dx and dy as well as di and dj. These last are obtained considering the direction of the line joining, for each hole, the centers on the two different planes.

3.6 Numerical results

3.6.1 Measurements

In Figure 5 the nominal values of the holes as well as the measured values relative to the three artifacts are reported. However, in order to allow to perceive the difference between nominal and measured values, the distances(dx,dy) of these ones with respect to their nominal values have been multiplied by a scaling factor of 300. Similarly in Figure 6 results relative to the orientation errors of the milled holes are reported. In each nominal position the sum of the orientation error vectors di and dj are reported for all three artifacts. In order to make such figure meaningful the vectors have been multiplied by a scaling factor of 10^4.

These figures clearly show that there is a consistent systematic error, but they also show that there is a systematic difference between measurements on the three artifacts. Moreover for what concerns Artifact 3 it appears that the measurements relative to the holes 12, 17, 23, 24, and 30 could be regarded as outliers.

Using the differences between nominal values of x,y coordinates and measured ones as well as the differences between the nominal and the measured orientation of the hole center line it is possible to identify the parameters of the polynomial models used to represent the total closed loop errors dx, dy, di, dj. As previously discussed, such polynomial models have particular structures according to relations (2) and (3); their complexity increases together with the degree of the polynomials used to represent satisfactorily the elementary error functions associated to the movement of each axis, which in relation (2) are indicated with the letters T(translational), R(Rotational) and S(Squareness). According to the a priori available information, this whole experiment was designed assuming that 5^{th} order degree polynomials satisfactorily represent such elementary error functions (for the elementary error function R_{XZ}, as previously discussed, the order of the polynomial is assumed one degree lower). The experimental data in Figures 5 and 6, however suggest that less complex functions could also enable a satisfactorily error identification.

Total closed loop error polynomial models have been therefore computed for different degrees of the elementary functions. The parameters of such closed loop error models have been estimated using ordinary least squares which, by definition, minimize the sum of the squares of the difference between the measured error and the one predicted by the model in each one of the 36 measurement points. Such cost function has been also used as criterion to evaluate the goodness of the error identification which can be achieved with the different models thus comparing their performances.

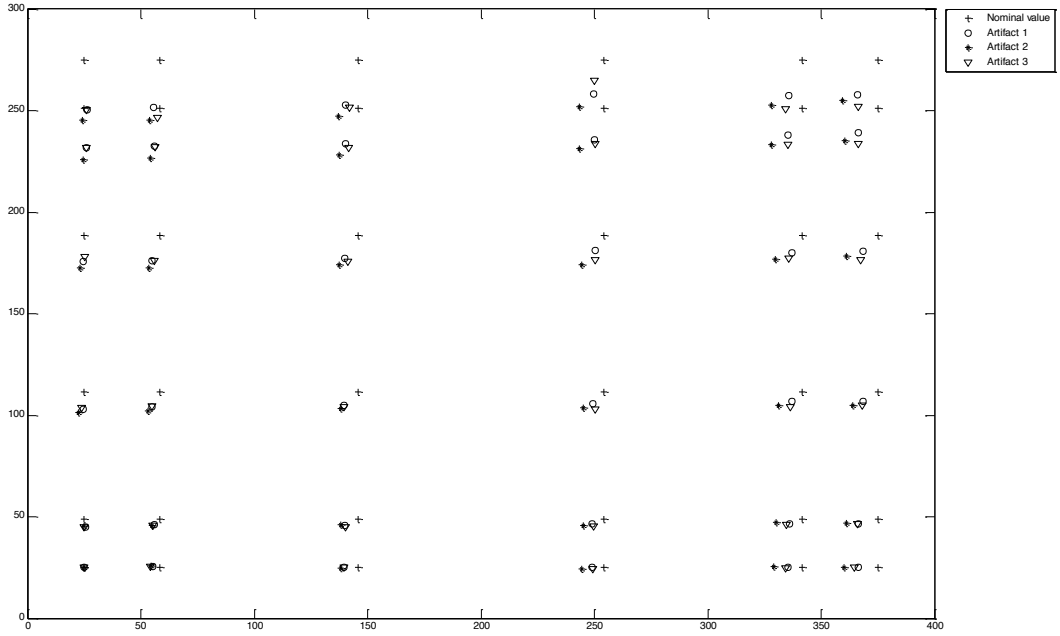

Figure 5: Nominal and measured values of the x,y coordinates of the hole centers for the three Artifacts. The distance between nominal values and measured ones has been multiplied by a scaling factor of 300.

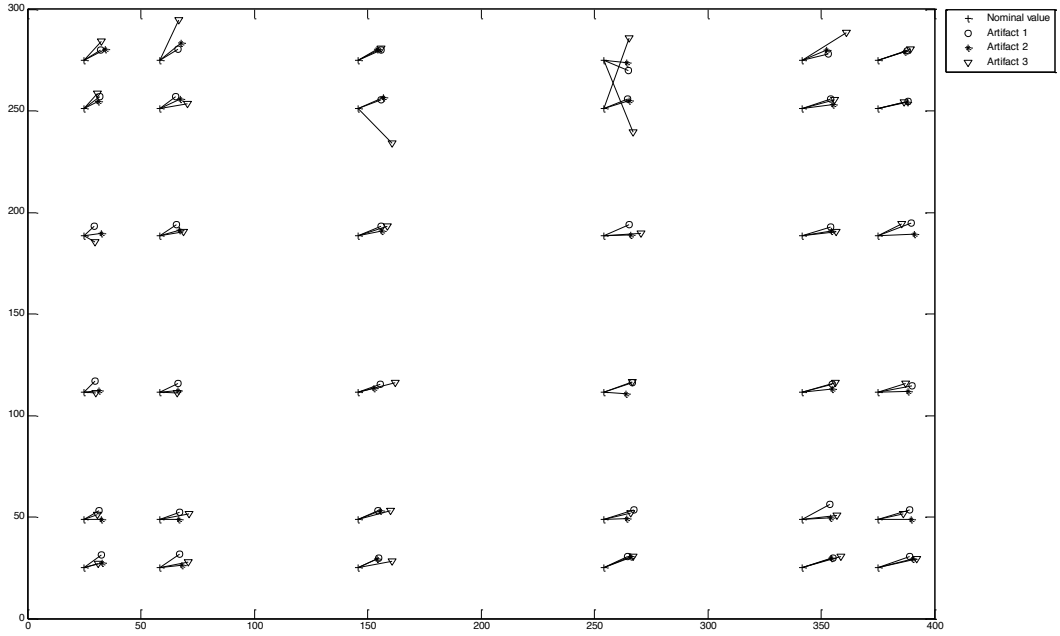

Figure 6: Nominal values of the x,y coordinates of the hole centers together with the vectors di+dj which account for the hole orientation error for the three Artifacts. The vectors have been multiplied by a scaling factor of 10^4.

3.6.2 Computation of Prediction errors

In Table 3 and in Table 4 the obtained average prediction error relative to the estimates of the total error functions for the three artifact is reported for different values of the degree assumed by the polynomials describing the elementary error functions. The average prediction error is the square root of the cost function (sum of square errors) once this last has been divided by the number of measurement points, which in our case is 36. In the tables the average prediction error without any correction is also reported for reference.

Table 3. Average prediction error for dx and dy using different model structures of increasing complexity

Degree of polynomials describing elementary error functions	Prediction error for dx			Prediction error for dy		
	Artifact 1	Artifact 2	Artifact 3	Artifact 1	Artifact 2	Artifact 3
No Correction	$1.7345 \cdot 10^{-2}$	$3.1355 \cdot 10^{-2}$	$1.7753 \cdot 10^{-2}$	$3.9523 \cdot 10^{-2}$	$5.0603 \cdot 10^{-2}$	$4.4751 \cdot 10^{-2}$
Degree 0	$8.9663 \cdot 10^{-3}$	$1.5087 \cdot 10^{-2}$	$9.5962 \cdot 10^{-3}$	$2.4782 \cdot 10^{-2}$	$3.1801 \cdot 10^{-2}$	$2.7647 \cdot 10^{-2}$
Degree 1	$5.2970 \cdot 10^{-3}$	$4.4895 \cdot 10^{-3}$	$4.6099 \cdot 10^{-3}$	$5.9212 \cdot 10^{-3}$	$5.9165 \cdot 10^{-3}$	$8.6133 \cdot 10^{-3}$
Degree 2	$4.8630 \cdot 10^{-3}$	$3.9396 \cdot 10^{-3}$	$4.4981 \cdot 10^{-3}$	$5.2275 \cdot 10^{-3}$	$5.3594 \cdot 10^{-3}$	$8.2658 \cdot 10^{-3}$
Degree 3	$1.9618 \cdot 10^{-3}$	$2.6312 \cdot 10^{-3}$	$2.0022 \cdot 10^{-3}$	$4.2626 \cdot 10^{-3}$	$4.8238 \cdot 10^{-3}$	$7.6195 \cdot 10^{-3}$
Degree 4	$1.9272 \cdot 10^{-3}$	$2.5492 \cdot 10^{-3}$	$1.9514 \cdot 10^{-3}$	$4.2603 \cdot 10^{-3}$	$4.8148 \cdot 10^{-3}$	$7.5230 \cdot 10^{-3}$
Degree 5	$1.9105 \cdot 10^{-3}$	$2.5316 \cdot 10^{-3}$	$1.9096 \cdot 10^{-3}$	$4.1502 \cdot 10^{-3}$	$4.8134 \cdot 10^{-3}$	$7.4376 \cdot 10^{-3}$

Table 4. Average prediction error for di and dj using different model structures of increasing complexity

Degree of polynomials describing elementary error functions	Prediction error for d1			Prediction error for dj		
	Artifact 1	Artifact 2	Artifact 3	Artifact 1	Artifact 2	Artifact 3
No Correction	$1.0693 \cdot 10^{-2}$	$1.0864 \cdot 10^{-2}$	$1.2593 \cdot 10^{-2}$	$4.9419 \cdot 10^{-3}$	$3.3891 \cdot 10^{-3}$	$1.0363 \cdot 10^{-2}$
Degree 0	$2.8536 \cdot 10^{-3}$	$2.5467 \cdot 10^{-3}$	$3.6597 \cdot 10^{-3}$	$1.8619 \cdot 10^{-3}$	$2.2164 \cdot 10^{-3}$	$9.7720 \cdot 10^{-3}$
Degree 1	$8.9155 \cdot 10^{-4}$	$1.2160 \cdot 10^{-3}$	$2.7363 \cdot 10^{-3}$	$1.7647 \cdot 10^{-3}$	$2.0820 \cdot 10^{-3}$	$9.7589 \cdot 10^{-3}$
Degree 2	$8.7390 \cdot 10^{-4}$	$1.1671 \cdot 10^{-3}$	$2.1943 \cdot 10^{-3}$	$1.7010 \cdot 10^{-3}$	$1.7043 \cdot 10^{-3}$	$9.7033 \cdot 10^{-3}$
Degree 3	$8.2505 \cdot 10^{-4}$	$1.0127 \cdot 10^{-3}$	$2.0896 \cdot 10^{-3}$	$1.5813 \cdot 10^{-3}$	$1.5626 \cdot 10^{-3}$	$9.6984 \cdot 10^{-3}$
Degree 4	$8.2489 \cdot 10^{-4}$	$1.0013 \cdot 10^{-3}$	$1.7703 \cdot 10^{-3}$	$1.5651 \cdot 10^{-3}$	$1.5110 \cdot 10^{-3}$	$9.6240 \cdot 10^{-3}$
Degree 5	$7.9607 \cdot 10^{-4}$	$9.5768 \cdot 10^{-4}$	$1.6824 \cdot 10^{-3}$	$1.5460 \cdot 10^{-3}$	$1.3917 \cdot 10^{-3}$	$9.5766 \cdot 10^{-3}$

From Table 3 it appears that, for what concerns the position errors dx and dy, model structures derived assuming third order polynomials for the description of elementary error functions adequately describe the measured errors. This can be verified looking at Figures 7a, 7b, 7c in which the nominal coordinates of the holes are reported together with the measured and the estimated ones which are the values that are computed adding to the nominal coordinates the errors dx and dy which are computed using the estimated parameters. Also in these figures the distance between nominal values on one side and measured and estimated values on the other has been multiplied by a scaling factor of 300 to make the differences visible.

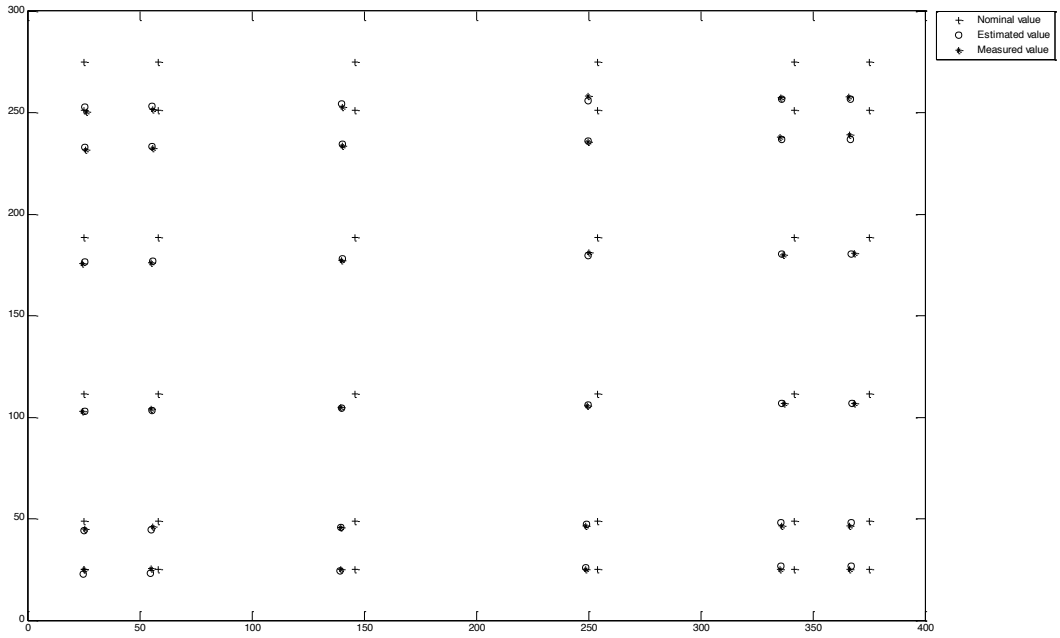

Figure 7a: Nominal values of the x,y coordinates of the hole centers together with the measured coordinates and the estimated ones using the models derived assuming third order polynomials for the descriprion of elementary errors. Data are relative to Artifact 1

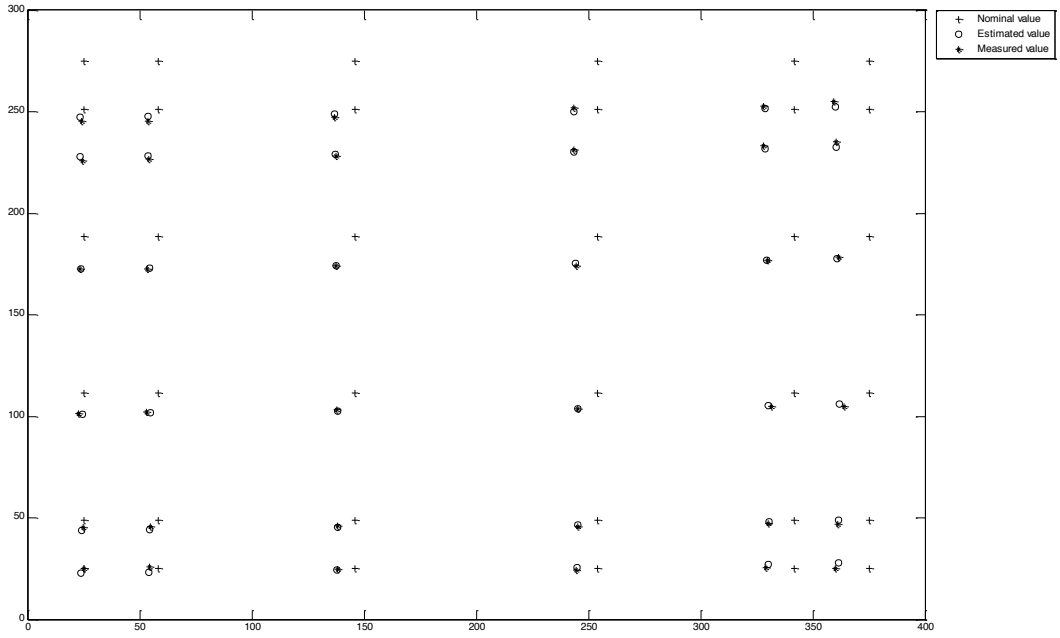

Figure 7b: Nominal values of the x,y coordinates of the hole centers together with the measured coordinates and the estimated ones using the models derived assuming third order polynomials for the descriprion of elementary errors. Data are relative to Artifact 2

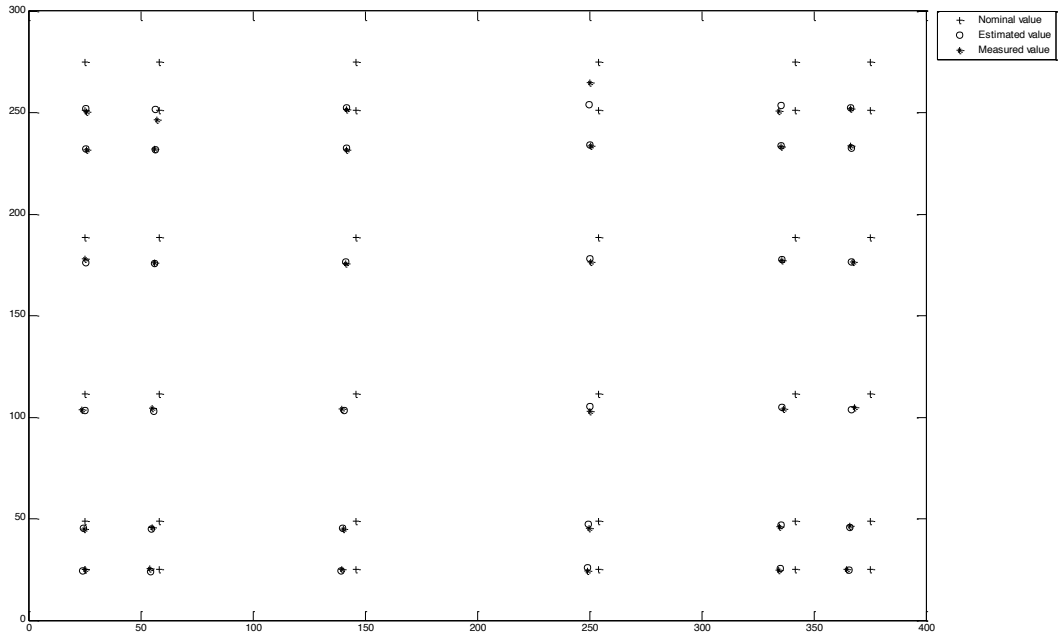

Figure 7c: Nominal values of the x,y coordinates of the hole centers together with the measured coordinates and the estimated ones using the models derived assuming third order polynomials for the description of elementary errors. Data are relative to Artifact 3

From Table 4 it appears that, for what concerns the orientation errors di and dj, model structures derived assuming first order polynomials for the description of elementary error functions adequately describe the measured errors. This can be verified looking at Figures 8a, 8b, 8c in which the nominal coordinates of the holes are reported together with the measured and the estimated vectors di+dj which account for the hole orientation error. Estimated vectors di and dj are computed using the estimated parameters. Also in these figures the vectors have been multiplied by a scaling factor of 10^4 for clarity of representation.

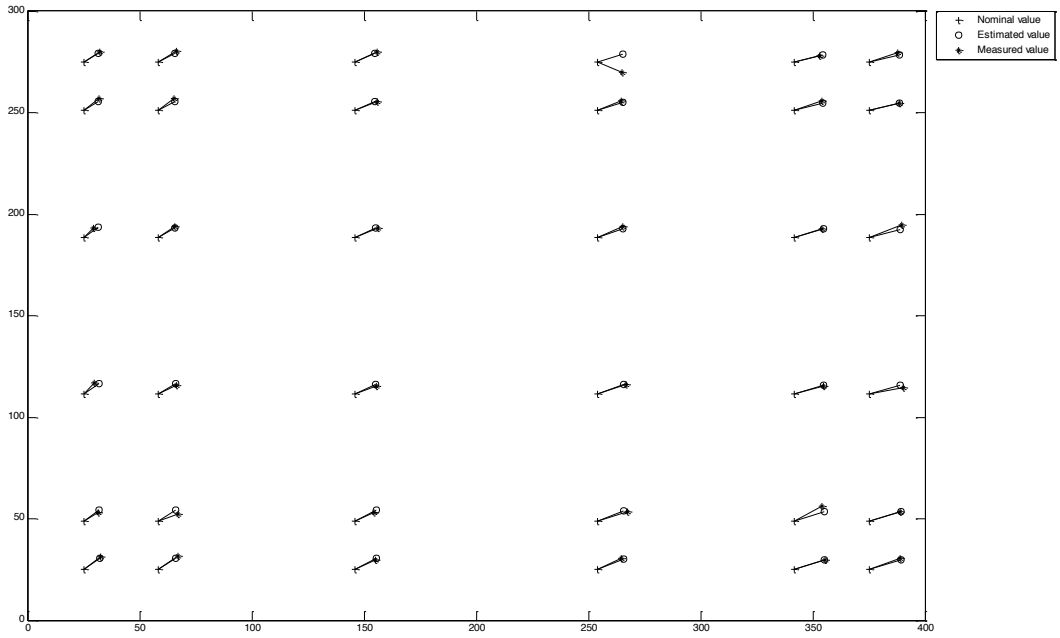

Figure 8a: Nominal values of the x,y coordinates of the hole centers together with the measured vectors di+dj and the estimated ones which are computed using their error models derived assuming first order polynomials for the descriprion of elementary errors. Data are relative to Artifact 1

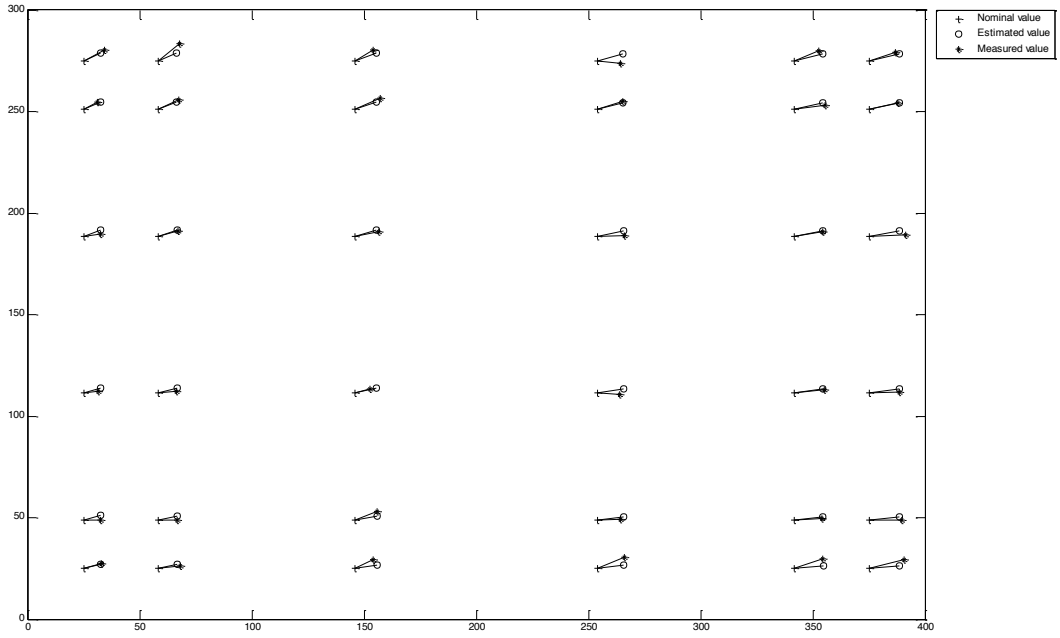

Figure 8b: Nominal values of the x,y coordinates of the hole centers together with the measured vectors di+dj and the estimated ones which are computed using their error models derived assuming first order polynomials for the descriprion of elementary errors. Data are relative to Artifact 2

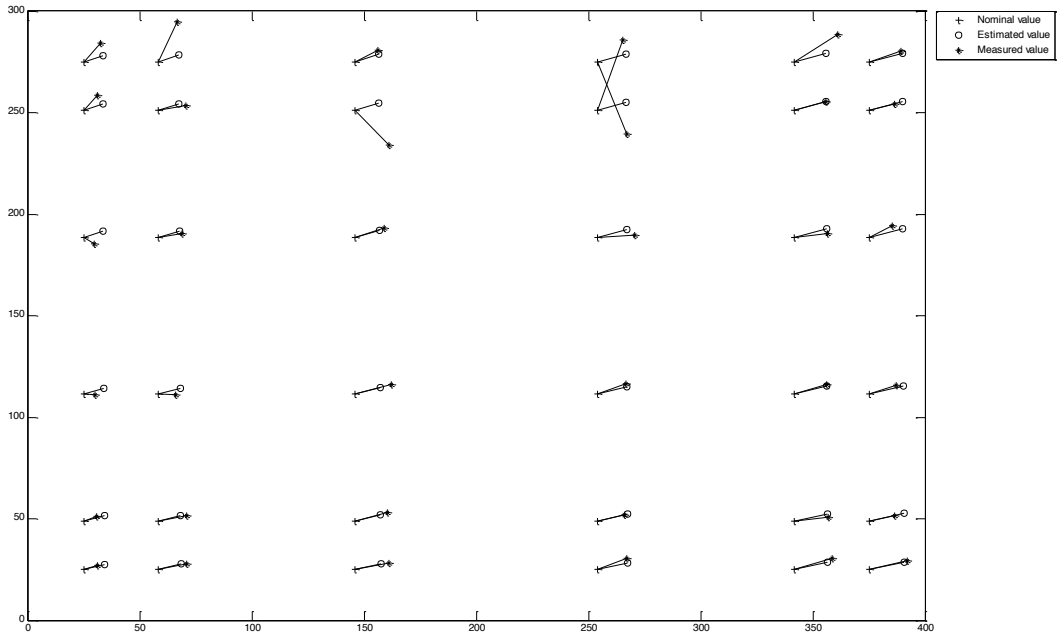

Figure 8c: Nominal values of the x,y coordinates of the hole centers together with the measured vectors di+dj and the estimated ones which are computed using their error models derived assuming first order polynomials for the descriprion of elementary errors. Data are relative to Artifact 3

3.6.3 Compensation for thermal Expansion

Indeed all the above reported results clearly show that total closed loop errors can be quite well identified from the measurements in all three artifacts. However, as noted before, there is a consistent systematic difference in the location of the holes in the three artifact. Such difference should be explained and possibly compensated if the procedure we are proposing and testing for CNC machine systematic error compensation has to be considered a valuable solution.

A possible reason for such differences could be related to changes in temperature. Actually the milling of the three artifacts required about 40 minutes. The solid piece used for the milling had been for several hours in the AIT lab where the milling machine is operated so that its temperature at the milling time can be assumed almost constant during the whole milling process. On the other hand, instead, the measurement process requires much more time. About 4 hours are required for measuring all the holes of one artifact only. Moreover the lab in which such measurement were carried on in Ho Chi Min City has no temperature control and the workpiece was most likely not in termal equilibrium with the environment.

Unfortunately at the time in which the experiments were conducted the available information suggested that the influence of temperature is negligible while later on it was figured out that this material has and ecpansion coefficient of 50 10^{-6}/°C so that a change in temperature of a few degrees like the one that could easily have occurred during the measurement of the artifacts can affect significantly the measurement. Unfortunately in the measurement lab that was used no recording of temperature data is available for the time in which measurements were carried on. However, in order to test whether a change in temperature could satisfactorily account for the systematic difference among the measurements of the three artifacts, it has been hypnotized that they have been measured at three different temperatures. With this hypothesis the difference in temperature between the measurements of artifact 1 and artifact 2 as well as between artifact 1 and artifact 3 have been estimated from the available data. The measurements of artifact 2 and of artifact 3 have then been compensated according the estimated changes and the obtained values are compared to the measurements of artifact 1 in In Figures 9a and 9b.

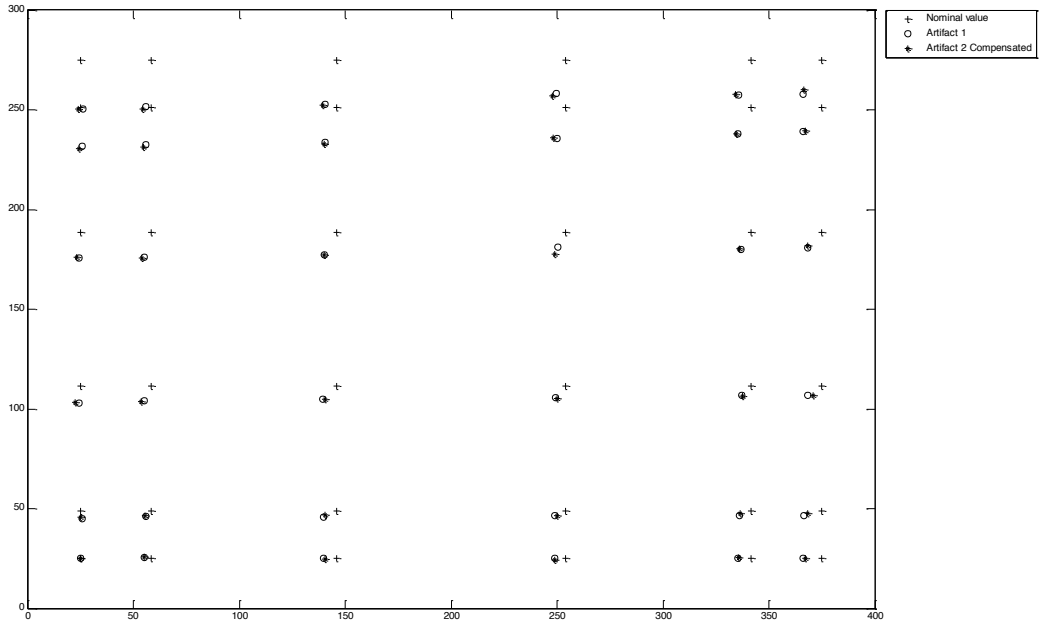

Figure 9a: Nominal values of the x,y coordinates of the hole centers together with the measured coordinates for Artifact 1 and those compensated for temperature of Artifact 2. The distance between nominal values on one side and measured or compensated ones on the other, has been multiplied by a scaling factor of 300.

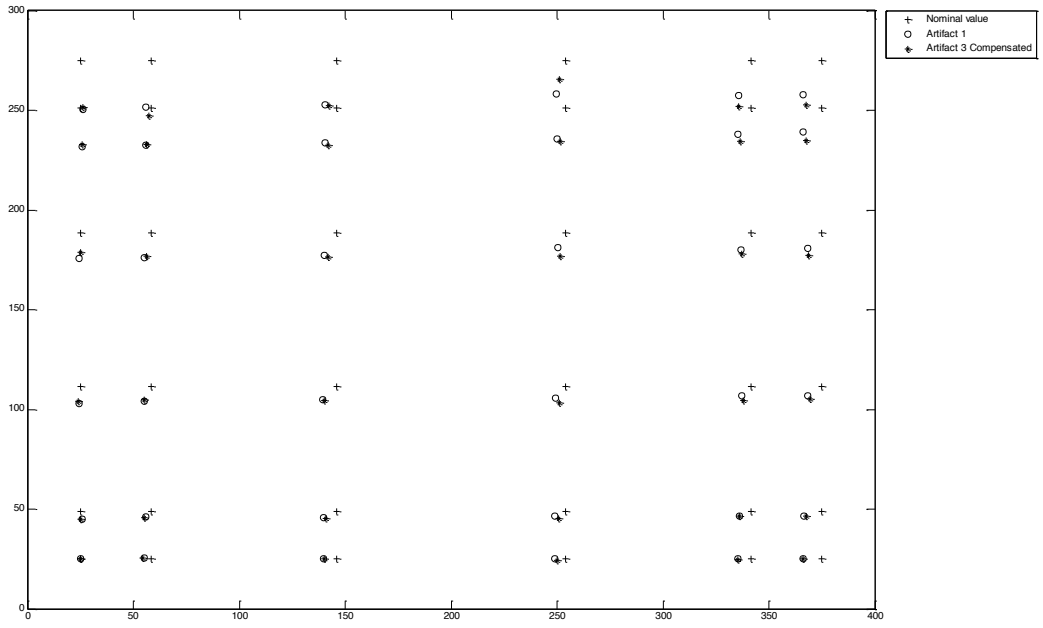

Figure 9b: Nominal values of the x,y coordinates of the hole centers together with the measured coordinates for Artifact 1 and those compensated for temperature of Artifact 3. The distance between nominal values on one side and measured or compensated ones on the other, has been multiplied by a scaling factor of 300.

3.6.4 **Assessment of the experiment**

The above experiments show that we can identify the systematic error for a 2-axis CNC machine tool with the new proposed method. When the measurement error bounds are normalized to one so that $|e(t)| \leq E=1$, the worst case prediction error that can be achieved within the normalized working space is quite consistent if measurements are reduced to a minimum (as many measurements as parameters) even in the case of optimal sampling choices when it equals 9 and 8.44. This worst case prediction error drops to 1.99 if all the 36 points of the optimal parameter estimation grid are used, and it drops further to 1.68 if the optimal prediction error grid is used. On the contrary the worst case prediction error would be 3.11 if a uniform gridding is used. The actual prediction error should be smaller than the worst case one since the used measurements are more than the parameters to be estimated.

The degree of the polynomials to model the systematic errors can be reduced from 5^{th} to 3^{rd}, making the method even more efficient by reducing the number of holes per axis to 4. The practical feasibility has been proven for the case study. However to extend the procedure to 3, 4 -axis CNC machines seems to be possible, as the number of holes will increase to respectively 64 and 254 in the case of 3^{th} Degree polynomials. The relation between the actual number of measurements (holes) and the worst case prediction error for the 5-axis case will need to be investigated further as probably the number of holes is rather high. The relation between reducing the number of holes and the worst case prediction error need to be investigated further for the case.

4 CONCLUSIONS

Aim of this paper is to contribute to the evaluation of the practical feasibility of a procedure to compensate systematic errors in CNC milling machine. The procedure is based on the idea to mill an artifact with the machine to be corrected and then to measure such artifact. The difference between nominal values of the artifact and measured ones allow to identify the systematic errors.

A new artifact based method to identify the systematic errors in multi-axis CNC machine tools minimizing the worst case prediction error is presented. The physical artifact is manufactured on the machine tool and later measured on a Coordinate Measuring Machine. The artifact consists of a set of holes at locations that minimize the worst case prediction error. The physical artifact in the experiment contained multiple virtual artifacts. This allowed to separate the random errors from the systematic errors and assess their relative magnitude. Also there was no additional random set up error for each atifact due to the combination in a single physical part. The result of the measurements is then used to compute the systematic error approximated as 5^{th} degree polynomials. A case study on a vertical milling machine is used to verify the new approach. It is observed that the degree can be lowered to three without reducing the systematic error estimates. The obtained results are very promising. The method is inherently simple and required only a short time to produce the artifact. The method is very simple because of three reasons. First only the six components of the closed loop systemactic error are measured directly. Secondly because the artifact consist only of producing holes. Thirdly because everything indicated that third degree polynomial are sufficient, the numbers of holes required per machine axis can be further reduced from 6 to 4.

The worst case prediction error drops to 1.99 if all the 36 points of the optimal parameter estimation grid are used, and it drops further to 1.68 if the optimal prediction error grid is used. On the contrary the worst case prediction error rises to 3.11 if a uniform gridding is used.

Further research will focus on repeating the experiment on different machines and higher number of axes. The measurements on the CMM machine did not use the canned cycles for the measurement of the hole to avoid additional error. It will also be investigated in the future.

5 REFERENCES

[1] Bohez E. L. J., Ariyajunya B., Sinlapeecheewa C., Shein T. M. M., Lap D. T., Belforte G.. Systematic geometric rigid body error identification of 5-axis milling machines. Computer-aided Design, 2007, 39, 229-244.

[2] Patent Title: Procedimento per l'identificazione e la compensazione degli errori sistematici in macchine utensili multi-asse a controllo numerico e relativo sistema. Application number N. TO2008A000512 (Italy) Application date 30-06-2008. Patent holder: Politecnico di Torino. Inventors: Gustavo Belforte, Erik L. J. Bohez.

[3] Patent Title: Procedimento per l'identificazione e la compensazione degli errori sistematici in macchine utensili multi-asse a controllo numerico e relativo sistema. Application number N. TO2009A001052 (Italy) Application date 29/12/2009. Patent holder: Politecnico di Torino. Inventors: Gustavo Belforte, Erik L. J. Bohez.

[4] N. V. Chung, G. Belforte, Erik L. J. Bohez. Minimal worst case optimal sampling for systematic angular error identification in multi-axis CNC machine tools. Proc. 20th International Conference on Production Research ICPR-20, Shanghai China, Serial No. 9.1 (CD), ISRC CN-E16-09-0006-0/A•H, August 2009.

[5] Schwenke H, Knapp W, Haitjema H, Weckenmann A, Schmitt R, Delbressine F (2008) Geometric error measurement and compensation of machines—an update. CIRP Annals Manuf Technol 57:660–675

[6] Patent Title: Method of assessing three dimensional volumetric errors in multiaxis machine tools. Patent number N. US5841668. Patent Assignee: Nat Univ Seul, SNU Precision Co LTD. Inventors: Pahk Heui Jae, Moon Joon Hee, Chu Chong Nam

[7] E. L. J. Bohez, Five–axis milling machine tool kinematic chain design and analysis. International Journal of Machine Tools & Manufacture, 42 (2002) 505-520.

[8] Belforte G., Bona B., Frediani S.. Optimal sampling schedule for parameter estimation of linear models with unknown but bounded measurement errors. IEEE Transactions on Automatic Control, 1987, AC-32, No. 2, 179-182.

[9] G. Belforte, P. Gay., Monegato G., Optimal sampling schedule for models with l_2 and l_∞ set membership errors. Proc. 36th Conference on Decision and Control, San Diego, California, pp. 744-749, December 1997.

[10] G. Belforte, P. Gay. Optimal experiment design for regression polynomial models identification. The International Journal of Control, 2002, 75, No. 15, 1178-1189.

[11] S.N. Bernstein, Sur la limitation des valeurs d'une polynome P(x) de degré n sur tout un segment par ses valeur en (n+1) points du segment, *Izv. Akad. Nauk,* SSSR 7, (1931), 1025-1050.

[12] A.T. Kilgore, A characterization of the Lagrange interpolating projection with minimal Tchebycheff norm, *Journal of approximation theory*, 24, (1978), 273-288.

[13] C. de Boor, A. Pinkus, Proof of the conjectures of Bernstein and Erdös concerning the optimal nodes for polynomial interpolation, *Journal of approximation theory*, 24, (1978), 289-303.

[14] G. Belforte, P. Gay. Optimal experiment design for regression polynomial models identification. The International Journal of Control, vol.75, No. 15, pp. 1178-1189, 2002.